J Therm Anal Calorim (2012) 109:403–412
DOI 10.1007/s10973-011-1556-z

Kinetics investigation on the combustion of waste capsicum stalks in Western China using thermogravimetric analysis

Xuebin Wang · Jipeng Si · Houzhang Tan · Yanqing Niu · Chao Xu · Tongmo Xu

Received: 5 February 2011 / Accepted: 31 March 2011 / Published online: 11 April 2011

Abstract The combustion kinetics of waste capsicum stalk (WCS) in Western China is investigated through thermogravimetric analysis compared with sawdust and coal, and co-combustion of WCS with coal is also investigated. Results show that the ignition characteristics of WCS is better than that of sawdust and coal, and the activation energy E of WCS-volatile combustion and WCS-char combustion are 78.55 kJ mol^{-1} and 44.59 kJ mol^{-1}. However, integrating the characteristics of ignition and burnout, the combustion characteristic factor (S_N) of WCS is lower than that of sawdust. With the increasing in the heating rate, the ignition of WCS is delayed. Oxygen concentration C_{O_2} affects E and k_0 of volatile combustion largely under rich-oxygen condition, when C_{O_2} increases from 0.2 to 0.8, E has increased threefold and k_0 also intensively increases from 10^6 to 10^{13}–10^{22}. Oppositely, effect of C_{O_2} on the E and k_0 of char combustion is little, and there is an exponential relationship $S_N = 7.128 \times 10^{-9} \times \exp(C_{O_2}/0.368) - 6.126 \times 10^{-9}$ between S_N and C_{O_2}. For the tests of co-combustion, all the experimental and weighted-average curves coincide well, and there is no remarkable synergistic effect. With the increase of mixing ratio that WCS added, E and k_0 of volatile combustion increase, but correspondingly E and k_0 of char combustion decrease.

X. Wang · J. Si · H. Tan (✉) · Y. Niu · C. Xu · T. Xu
School of Energy and Power Engineering, Xi'an Jiaotong University, Xi'an 710049, China
e-mail: xuebin.wang@berkeley.edu

X. Wang
Department of Mechanical Engineering, University of California at Berkeley, Berkeley, CA 94720, USA

Keywords Biomass · Co-combustion · Capsicum stalk · Thermogravimetric

Introduction

Humans have been using and benefiting from biomass for thousands of years, and with the aggravation of global greenhouse effect and energy shortage, biomass has been focused as a renewable fuel more and more. Biomass takes care of its own carbon dioxide emissions and mitigates acid rain for producing virtually no sulfur emissions [1–3]. However, due to the complex variety of biomass, there are abundant and unique problems during the combustion of different biomass.

Capsicum is one of the most common flavorings all around the world, and an important cash crop in the region of Western China. In India and Spain, the major producers of capsicum, there are million hectares of cultivated area for capsicum, and the capsicum yield is more than 1 million tons [4, 5]. Globally, the yield of hot pepper has reached 14–15 million tons per year [5]. In China, the planting of capsicum is mainly distributed in the western provinces, such as Shaanxi, Guizhou, Hunan, and Sichuan. Presently, the capsicum yield in China has reached up to 28 million tons in 1 year, accounting for about 46% of the world total output, with an increasing rate of 9% every year [6]. However, large area of capsicum-planting has brought much more waste capsicum stalk (WCS). Because of its peppery smell, WCS is hardly used for paper-making and forage-producing; consequently, it is suggested co-utilized with coal and other biomass in a 300 MW tangentially pulverized furnace of Baoji Power Plant, in Shaanxi Province, Western China [7]. The advantages of co-combustion also including: (a) reducing the costs of generating

electricity; (b) reducing C_{O_2} emission for greenhouse effect; (c) reducing SO_2, NO_x, and particulate emission [2, 8–10].

Before the successful and optimal co-combustion of WCS with coal, the combustion characteristics of WCS should be demonstrated clearly, whereas there is no report or data related to the combustion kinetics of WCS.

Thermogravimetric analysis (TG) method is mostly applied for the research of the combustion kinetics of solid fossil fuels including coal [11–15], coke [16–18], soot [19], waste [20–22], and all kinds of biomass [23–25]. Compared with fixed-bed reactor [26, 27] and other reactor [28] in the past, TG can accurately record the trivial behavior of mass loss during the reaction process for various techniques of thermal analysis, both under isothermal and temperature programmed condition [12, 29].

In this work, combustion kinetics of WCS is investigated using TG under the temperature programmed conditions. The combustion characteristic of WCS is compared with sawdust and Baoji coal; effects of O_2 concentration, particle diameter and heating rate on combustion characteristics and kinetics parameters are analyzed; and the co-combustion of WCS with Baoji coal is also investigated.

Coats-Redfern method [30–32] is employed to determine the kinetics parameters, considering the combustion mechanism of independent first order parallel reactions and assuming that intra-particle heat transfer and diffusion efforts are negligible. Furthermore, to systematically integrate the characteristics of ignition and burnout for combustion of solid fuels, combustion characteristic factor S_N has been applied to describe the process of WCS combustion better [33].

Experiments and theories

Sample preparation

The WCS used in experiment was from Fengxiang County, around Baoji Power Plant, in Shaanxi Province, Western China. After the fruitages and seeds removed from stalks in October last year, WCS has been collected and air dried for about 6 months. Sawdust and Baoji coal are prepared to compare with the combustion characteristic of WCS. Sawdust comes from a wood factory around Xi'an in Shaanxi Province, and Baoji coal is the coal powder ($D < 198$ μm) commonly used in Baoji Power Plant. The biomass sample (WCS and sawdust) were dried in oven for 24 h, then crushed and sieved below 2000 μm. The elemental analysis and proximate analysis of samples are listed in Table 1. It shows that the volatile in biomass (WCS and sawdust) is more than 70%, and volatile in Baoji coal is also high up to 37.66%, which should be classified as a high-quality bituminous coal. For each test, 6 ± 0.2 mg sample was weighted, and three particle diameter ranges (198–450, 450–1000, and 1000–2000 μm) were selected to investigate the effect of particle diameters. During tests for co-combustion of WCS and Baoji coal, two samples were well mixed mechanically and the mixing ratios of WCS in Baoji coal were selected as $\lambda = 0.1$, 0.2, and 0.4.

Table 1 Proximate analysis and elemental analysis of WCS, sawdust and Baoji coal

Sample	Proximate analysis/%			Elemental analysis/%				
	M_{ar}	A_{ar}	V_{daf}	C_{ar}	H_{ar}	N_{ar}	O_{ar}	S_{ar}
WCS	4.44	5.17	71.79	44.04	3.94	0.91	41.19	0.31
Sawdust	9.87	0.42	76.77	44.75	4.98	0.12	39.85	0.01
Baoji coal	7.38	19.10	37.66	57.89	3.34	0.60	10.98	0.71

TG analysis

TG analysis was performed on a thermal analyzer (Netzsch STA 409 PC), and its temperature range was from 298 to 1823 K, with heating rates from 0 to 50 K min^{-1} and weight precision of 0.01 mg. In the STA system, the sample was heated in a micro-furnace enclosed by a cooling jacket, and water was used as the cooling agent. The sample temperature was measured with a type S ($P_t - R_h/P_t$) thermocouple directly under the crucible (Al_2O_3). In the present experiments, combustion of the samples was carried out over a temperature range of 298–1673 K, at a heating rate of 30 K min^{-1}, and the total carrier gas flow (N_2 and O_2) is constant as 100 mL min^{-1}. Temperatures were controlled increasing linearly to obtain the corresponding TG and differential thermogravimetric (DTG) combustion curves. Three different heating rates ($\beta = 10$, 20, 30 K min^{-1},) were selected to investigate the effect of heating rates. The concentration of O_2 is changed between 0.1 and 0.8, and the combustion of WCS under oxygen-rich condition is investigated furthermore.

Kinetics model for combustion in TG

Heterogeneous combustion of solid fuels in TG can generally be described as: $A_{(s)} \rightarrow B_{(s)} + C_{(g)}$, and then the combustion rate of solid fuel sample A is expressed as:

$$\frac{d\alpha}{d\tau} = k(1-\alpha)^n \quad (1)$$

In which, α is the ratio of sample A consumed; τ is the reaction time; n is the reaction order of combustion; and reaction rate constant k is from the Arrhenius formula:

$$k = k_0 \exp\left(-\frac{E}{RT}\right) \quad (2)$$

where k_0 is the pre-exponential factor; E is the activation energy; R is the ideal gas constant; and T is instantaneous temperature.

The heating rate β is defined as:

$$\beta = \frac{dT}{d\tau} \tag{3}$$

Because β is kept constant during the linearly heating process, then the combustion rate should be further expressed as:

$$\frac{d\alpha}{dT} = \frac{k_0}{\beta}(1-\alpha)^n \exp\left(-\frac{E}{RT}\right) \tag{4}$$

Furthermore, integrating and converting Eq. 4 gives:

$$\int_0^{\alpha} \frac{d\alpha}{(1-\alpha)^n} = \frac{k_0}{\beta}\int_0^{T} \exp\left(-\frac{E}{RT}\right)dT \tag{5}$$

Coats-Redfern method [32] is employed to obtain the integral result of Eq. 5 in the form of natural logarithm [30] Eqs. 6 and 7:

$$\ln\left\{\frac{1}{n-1}\left[\frac{1}{(1-\alpha)^{n-1}}-1\right]\frac{1}{T^2}\right\} = \ln\left(\frac{k_0}{\beta}\frac{R}{E}\right) - \frac{E}{RT}(n \neq 1) \tag{6}$$

$$\ln\left[-\frac{\ln(1-\alpha)}{T^2}\right] = \ln\left(\frac{k_0}{\beta}\frac{R}{E}\right) - \frac{E}{RT}(n = 1) \tag{7}$$

Most of the literatures and data reported [12, 20, 34–41] have considered the pyrolysis and combustion of solid fuels as one order reaction, and then Eq. 7 is selected to describe the kinetics model for combustion of WCS, sawdust and Baoji coal. The kinetic parameters k_0 and E can be obtained from the plot of $\ln[-\ln(1-\alpha)/T^2]$ and $1/T$.

Combustion characteristic factor S_N

To systematically integrate the characteristics of ignition and burnout of solid fuels, Nie et al. [33] have introduced the combustion characteristic factor S_N ($mg^2\ min^{-2}\ K^{-3}$) to describe the process of coal combustion better.

$$S_N = \frac{(dw/d\tau)_{max}(dw/d\tau)_{mean}}{T_i^2 T_h} \tag{8}$$

In which, w is the residual sample mass (mg); $(dw/d\tau)_{max}$ is the maximum combustion velocity ($mg\ min^{-1}$); $(dw/d\tau)_{mean}$ is the average combustion velocity ($mg\ min^{-1}$); T_i is the ignition temperature (K) [34]; T_h is the burnout temperature (K) [34].

To express the role of S_N for combustion more intuitively, S_N can also be converted to another formula [33]:

$$S_N = \frac{E}{R}\frac{d}{dT}\left(\frac{dw}{d\tau}\right)_{T=T_i}\frac{(dw/d\tau)_{max}}{(dw/d\tau)_{T=T_i}}\frac{(dw/d\tau)_{mean}}{T_h} \tag{9}$$

where $\frac{R}{E}$ is related to the activity of solid fuels; $\frac{d}{dT}\left(\frac{dw}{d\tau}\right)_{T=T_i}$ is referring to the ignition intensity at the ignition temperature; $\frac{(dw/d\tau)_{max}}{(dw/d\tau)_{T=T_i}}$ shows the rate of combustion velocity at peak temperature and ignition temperature; $\frac{(dw/d\tau)_{mean}}{T_h}$ is the rate of average combustion velocity and burnout temperature, and burnout is improved with the increase of $\frac{(dw/d\tau)_{mean}}{T_h}$.

Consequently, S_N has systematically integrated the characteristics of ignition and burnout for combustion of solid fuels, and it should be more effective to express the characteristics of combustion. With the increasing of S_N, the combustion characteristics of solid fuels should be improved.

Results and discussion

Comparison of WCS with sawdust and Baoji coal

The TG and DTG curves for combustion of WCS, sawdust and Baoji coal have been depicted in Fig. 1. It can be seen that the ignition temperature of biomass (WCS-volatile and sawdust-volatile) is lower than that of Baoji coal for 100–150 K, and the process of biomass combustion is obviously divided into two stages, compared with only one stage for Baoji coal. Correspondingly, in Fig. 1 there are two peaks of mass loss for biomass and only one peak for Baoji coal, because the volatile in Baoji coal is much lower than that in biomass, then the peak of volatile combustion has been merged by the main peak of char combustion. In the second stage of biomass combustion, most of volatiles have emitted when temperature reaches about 700 K, and the fixed carbon catches fire, in this stage, the reactions including the continual emission of residual volatile and the combustion of char [23].

Even if the combustion process can be divided into two stages for both WCS and sawdust, however, there are still

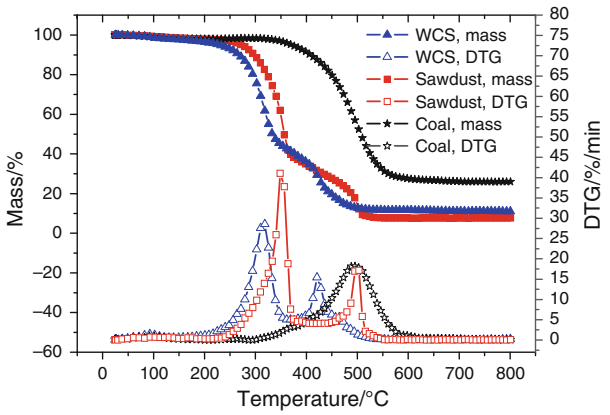

Fig. 1 TG and DTG curves of WCS, sawdust, and Baoji coal (β = 30 K min^{-1}; C_{O_2} = 0.2; particle diameters = 198–450 μm)

remarkable differences for the TG–DTG curves between WCS and sawdust. It shows that the ignition of WCS is better that that of sawdust, the first DTG peak of volatile combustion of WCS is ahead of that of sawdust by 36 K and the second DTG peak of char combustion of WCS is ahead of that of sawdust by 80 K in Table 2. The peak of char combustion for sawdust almost coincides with that of Baoji coal, which indicates that the combustion reactivity of sawdust char is similar with that of Baoji coal char.

The most significant natural factor affect the curve of TG and DTG should be from the component of the biomass. It is suggested that biomass mainly contains three components: hemicellulose, cellulose, and lignin [42], and researchers have also defined four main types of biomass: woody plants, herbaceous plants/grasses, aquatic plants, and manures. McKendry [43] and Gani [44] believes that the lignin content in wood can reach up to 30–35%, much higher than that in wheat-straw and switch-grass, and it is pointed out that the cellulose and lignin content in biomass is one of the important parameters to evaluate the pyrolysis and combustion characteristics. The reactivity of lignin is lower than that of cellulose, and less content of cellulose in sawdust can also decreases the porosity of biomass char to further inhibit the reactivity of biomass [44]. The content of lignin in sawdust (woody plants) should be obviously much higher than that in WCS (herbaceous plants), which due to the ignition delay for the sawdust compared with WCS.

Based on the linear regression method in Eq. 7, the data for $1/T$ and $\ln[-\ln(1-\alpha)/T^2]$ corresponding to volatile combustion and char combustion are filtered for fitting in Fig. 2. Then E and k_0 can be calculated, respectively, as shown in Table 2 corresponding to the linear fitting function and variance error. The statistical data shows that the activity energy E is in the same range for all the three fuel samples, and the T_i, T_f, and E of WCS is lower than that of sawdust, which demonstrates that WCS is easier to be ignited and burned. In contrast, the k_0 and E of sawdust is larger, which indicates that the combustion of sawdust is more sensitive to the change of temperature, and it also can be seen from Fig. 1, the peaks of sawdust are the sharpest, and once the sawdust is ignited, then it will be burned out in the fastest reaction velocity.

Effect of oxygen concentration, heating rate and diameter

Figure 3 illustrates the effect of oxygen concentration C_{O_2} on the combustion of WCS under the condition that β is 30 K min^{-1}, and particle diameter is 198–450 μm. As seen from Fig. 3, with the increase of C_{O_2} from 0.1 to 0.8, the ignition of biomass is improved obviously, and the mass loss from the first stage of TG curve increases from 50 to 85%; Fig. 3 shows that in the first stage, the combustion reactivity is exquisite and the maximum value of DTG curve under rich-oxygen condition is much higher than that under air condition and lean-oxygen condition. In the model of Janse [45] and Varhegyi [46], the combustion velocity is proportional to the 0.53th power of oxygen concentration, compared with 0.78th power in the model of Kashiwagi and Nambu [47]. When C_{O_2} reaches up to 0.8, the second DTG peak of char combustion would almost disappear, and Fang et al. [48] also proposes that there is critical C_{O_2} when the combustion process of wood varies from double stages to a single stage with C_{O_2} increasing.

The linear fitting of Arrhenius constants under different C_{O_2} has been shown in Fig. 4, and E and k_0 are calculated using the fitted coefficient, as listed in Table 3. E and k_0 for volatile combustion is always higher than that for char combustion, which agrees with that the peak of volatile combustion is much sharper than that of char combustion, and it means that volatile combustion is more sensitive to the temperature. With the increasing of C_{O_2} from 0.1 to 0.8, E and k_0 for volatile combustion increase intensely, however, the change of E and k_0 for char combustion is not very large: E is always around 42 kJ mol^{-1}, and k_0 is in the range of 10^2 to 10^3.

Especially for volatile combustion, the values of E and k_0 are totally different under the conditions of lean-oxygen and rich-oxygen: when C_{O_2} increases from 0.1 to 0.2, it is still under the condition of lean-oxygen or air condition,

Table 2 Kinetic parameters of combustion characteristics for different solid fuel samples

Sample	$T_i - T_f$/K	Linear fit	R	E/kJ mol^{-1}	k_0/min^{-1}	T_p/K
Sawdust volatile	598.6 – 636.4	$y = -12195x + 6.1829$	−0.99408	101.39	1.7722E+08	624.2
Sawdust char	761.3 – 781.8	$y = -14928x + 6.9962$	−0.98123	124.11	4.8925E+08	772.4
WCS volatile	555.6 – 606.6	$y = -9444.6x + 2.5976$	−0.99407	78.522	3.8056E+06	588.9
WCS char	685.5 – 729.2	$y = -5363.4x - 4.89428$	−0.99838	44.591	1.2050E+03	692.6
Baoji coal	703 – 819.2	$y = -10629x + 0.40086$	−0.99852	88.370	4.7611E+05	764.7

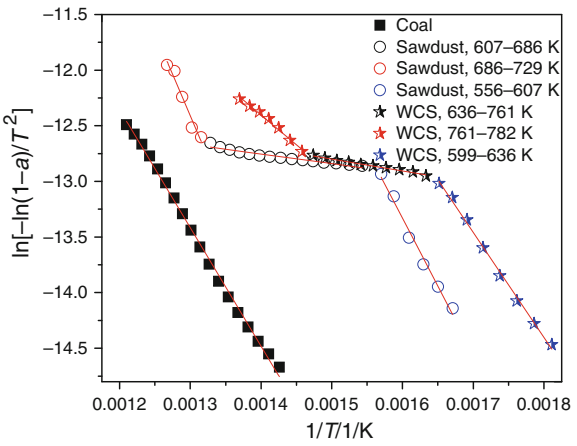

Fig. 2 Linear relationship for Arrhenius constant of WCS, sawdust, and Baoji coal ($\beta = 30$ K min^{-1}; $C_{O_2} = 0.2$; particle diameters = 198–450 μm)

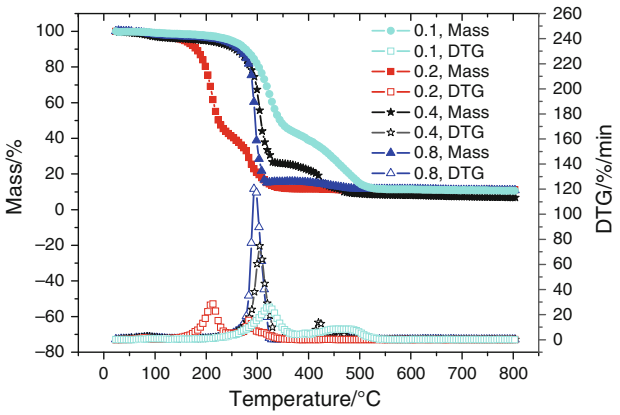

Fig. 3 Effect of oxygen concentration on TG and DTG curves of WCS ($\beta = 30$ K min^{-1}; particle diameters = 198–450 μm)

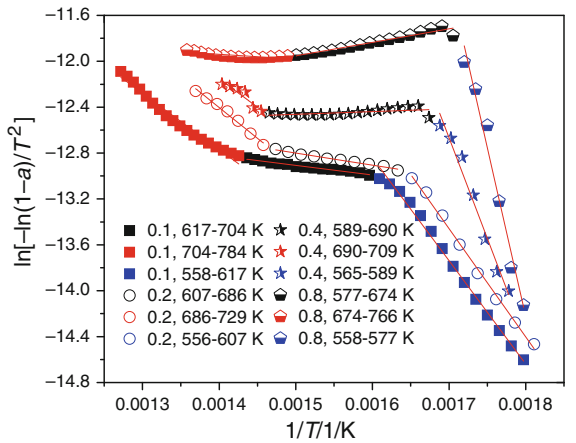

Fig. 4 Linear relationship of Arrhenius constant under different oxygen concentration (WCS; $\beta = 30$ K min^{-1}; particle diameters = 198–450 μm)

and then there is no much change of E and k_0; however, when C_{O_2} continually increases to 0.4 and 0.8, E has increased threefold, and k_0 also intensively increases from 10^6 to 10^{13}–10^{22}. Correspondingly it can be seen from Fig. 3, the TG curves of lean-oxygen and air condition coincide well, and TG curves of rich-oxygen condition have advanced more than that of lean-oxygen condition.

It is indicated that homogenous volatile combustion would be improved much under the rich-oxygen condition, in contrast, the increasing of C_{O_2} can only affect the heterogeneous char combustion little. It is because the reaction of char combustion is controlled by the diffusion of gas species in the char, however, the reaction of volatile combustion is mainly considered as a dynamics-control process.

Figures 5 and 6 have shown the effect of particle diameter and heating rate on the combustion curves of WCS. Three particle diameter ranges 198–450 μm, 450–1000 μm, and 1000–2000 μm have been selected to investigate the effect of particle diameters under the condition that C_{O_2} of 0.2 and β of 30 K min^{-1}. Figure 5 shows that the TG and DTG curves for three diameters almost coincides with each other, indicating that the effect of particle diameter on the combustion of WCS is really minor, which is consistent with previous results for biomass pyrolysis and combustion [49–51]. This should be the result of the competition between the effects of ash content and heating transfer. There is a temperature gradient inside the particle, and the increasing in particle size results to a lower core temperature, which inhibits the combustion reaction. However, it can be seen from Fig. 5, with the increasing in particle size, the residual ash ratio is reduced, which mainly due to the segregation during the shredding and sieving process, and it improves the combustion reaction [49]. Therefore, there is no remarkable different from the change of particle size.

Effect of heating rate on the combustion characteristics of WCS is investigated under three heating rate 10, 20, and 30 K min^{-1}. The TG–DTG curves in Fig. 6 show that with the increasing in the heating rate, the ignition of WCS is delayed, especially for the first stage of volatile combustion, even if the influences are not so remarkable for the second stage of char combustion and for the residual ratio. The ignition delay should be due to the thermal lag effect, because there is a temperature profile inside the biomass particle, under high heating rates, the temperature gradient increases, leading to a higher temperature needed for the combustion reaction [49, 52, 53].

Co-combustion of WCS with Baoji coal

Figure 7 has revealed the combustion characteristics of Baoji coal blended with WCS at different mixing ratios

Table 3 Effect of oxygen concentration on kinetic parameters of WCS combustion

C_{O_2}	$T_i - T_f$/K	Linear fit	R	E/kJ mol^{-1}	k_0/min^{-1}	T_p/K
0.1 volatile	557.7 – 616.9	$y = -8985.3x + 1.5366$	−0.99717	74.704	1.2531E+06	595.2
0.1 char	703.6 – 784.1	$y = -4898.7x - 5.9114$	−0.98691	40.728	3.9803E+02	732.0
0.2 volatile	555.6 – 606.6	$y = -9444.6x + 2.5976$	−0.99838	78.522	3.8056E+06	588.9
0.2 char	685.5 – 729.2	$y = -5363.4x - 4.89428$	−0.99407	44.591	1.2050E+03	692.6
0.4 volatile	564.6 – 588.6	$y = -17547x + 17.164$	−0.98927	145.89	1.4981E+13	577.8
0.4 char	689.6 – 709.0	$y = -4966.8x - 5.1986$	−0.93876	41.294	8.2314E+02	694.5
0.8 volatile	557.9 – 577.4	$y = -29470x + 38.820$	−0.98938	245.01	6.3946E+22	568.4
0.8 char	–	–	–	–	–	–

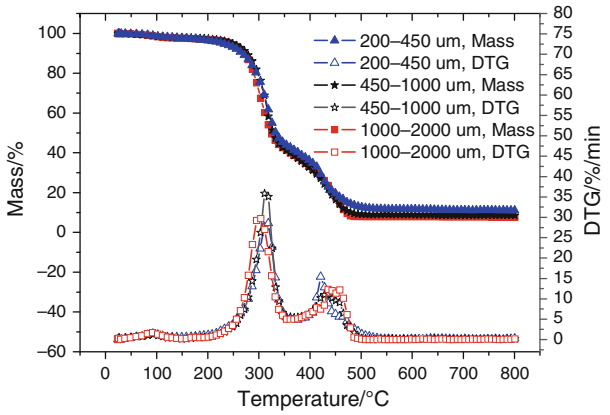

Fig. 5 Effect of particle diameter on TG and DTG curves of WCS (β = 30 K min^{-1}; C_{O_2} = 0.2)

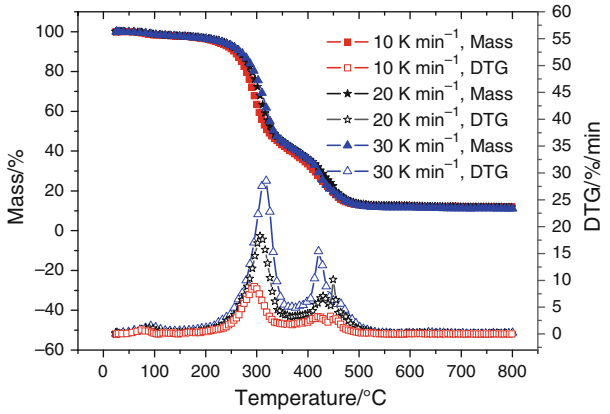

Fig. 6 Effect of heating rate on TG and DTG curves of WCS (particle diameters = 198–450 μm; C_{O_2} = 0.2)

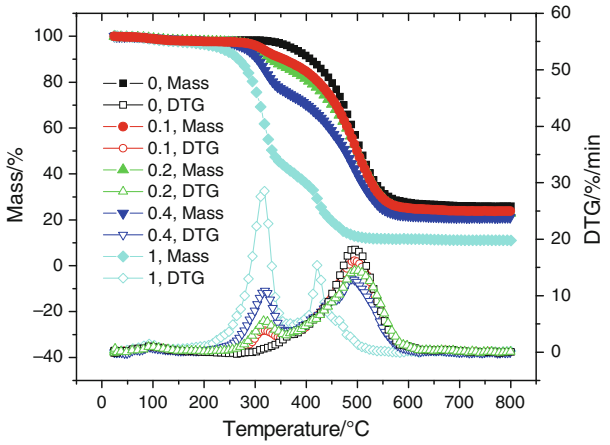

Fig. 7 TG and DTG curves for combustion of Baoji coal blended with WCS at different mixing ratios: 0, 0.1, 0.2, 0.4, 1 (β = 30 K min^{-1}; particle diameters = 198–450 μm; C_{O_2} = 0.2.)

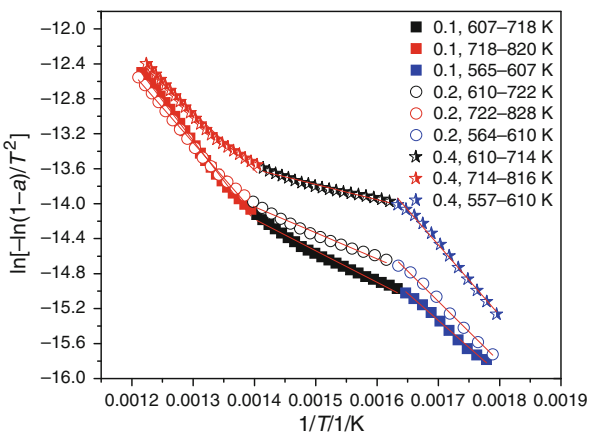

Fig. 8 Linear relationship of Arrhenius constant for blended sample combustion with different mixing ratio (Baoji coal blended with WCS; β = 30 K min^{-1}; C_{O_2} = 0.2; particle diameters = 198–450 μm)

under the condition that β of 30 K min^{-1}, particle diameters of 198–450 μm and C_{O_2} of 0.2. As seen from Fig. 7, with the increasing of biomass mixing ratio, the residual mass decreases gradually, and the TG curve shifts to a lower temperature scope, especially, the shift is more obvious in the first stage of volatile combustion when temperature is lower than 700 K. Figure 7 show that during the combustion process of Baoji coal blended with WCS, there are always two peaks in the DTG curves. The first peak is mainly due to the combustion of WCS-volatile, and

Table 4 Effect of λ on kinetic parameters of Baoji coal combustion blended with WCS

λ	$T_i - T_f$/K	Linear fit	R	E/kJ mol^{-1}	k_0/min^{-1}	T_p/K
0 coal	703.0 – 819.2	$y = -10629x + 0.40086$	−0.99852	88.370	4.7611E+05	764.7
0.1 volatile	565.2 – 606.9	$y = -6170.3x - 4.8455$	−0.99703	51.300	1.4556E+03	591.3
0.1 char	718.2 – 819.6	$y = -9166.4x - 1.3618$	−0.99828	76.209	7.0453E+04	767.1
0.2 volatile	563.6 – 610.1	$y = -6929.3x - 3.3377$	−0.99739	57.610	7.3836E+03	589.9
0.2 char	721.7 – 827.7	$y = -8056.3x - 2.82946$	−0.99731	66.980	1.4270E+04	772.3
0.4 volatile	557.2 – 610	$y = -8070.3x - 0.7511$	−0.99694	67.096	1.1424E+05	592.4
0.4 char	713.8 – 816	$y = -6593.6x - 4.3856$	−0.99322	54.819	2.4638E+03	761.4
1 volatile	555.6 – 606.6	$y = -9444.6x + 2.5976$	−0.99407	78.522	3.8056E+06	588.9
1 char	685.5 – 729.2	$y = -5363.4x - 4.89428$	−0.99838	44.591	1.2050E+03	692.6

the second peak is due to the combustion of coal char. For the mixing ratio scope (0.1–0.4) in experiments, the peak of WCS-char combustion cannot be seen from the DTG curve, and it means that this peak has been merged by the main peak of coal char combustion. It is because the content of fixed carbon in WCS is much lower than that in Baoji coal, furthermore, seen from Fig. 1, the combustion reactivity of WCS-char is higher than coal and sawdust, and its peak temperature is also much lower.

Figure 8 gives the linear relationship between kinetics constant and temperatures under the different λ of WCS blended in Baoji coal, and the data fit in line well with small error. The kinetic parameters in Table 4 illustrate that with the increase of λ, E, and k_0 of volatile combustion increase, but correspondingly E and k_0 of char combustion decrease. It is indicated that with λ increasing, the volatile combustion is more sensitive to the change of temperature, due to the enhancement of volatile content in blended fuels, but char combustion will be more insensitive to temperature changing.

To further investigate whether there is interactions existed between the combustion of coal blended with WCS, the theoretical TG and DTG curves are calculated, which represent the sum of the individual mass loss from different fuels as weighted average.

For TG curves:

$$\alpha_{\text{sum,weighted-average}} = \lambda\alpha_{\text{WCS}} + (1-\lambda)\alpha_{\text{Baoji-coal}} \quad (10)$$

For DTG curves:

$$\left(\frac{\mathrm{d}\alpha}{\mathrm{d}\tau}\right)_{\text{sum,weighted-average}} = \lambda\left(\frac{\mathrm{d}\alpha}{\mathrm{d}\tau}\right)_{\text{WCS}} + (1-\lambda)\left(\frac{\mathrm{d}\alpha}{\mathrm{d}\tau}\right)_{\text{Baoji-coal}} \quad (11)$$

In which, α_{WCS} and $\alpha_{\text{Baoji coal}}$ are the ratio of mass consumed from the results of individual experiments; λ and $1 - \lambda$ mean the mass fraction of WCS and Baoji coal in the blended fuels.

The experimental and calculated curves with different mixing ratios are illustrated in Fig. 9, and results show that the experimental values and calculated values coincide well for both TG and DTG curves, which means there is no remarkable synergistic effect for all the three co-combustion cases in the experiments, and the co-combustion characteristics can be treated as the single plus results between two fuels. This result is consistent with previous results on biomass co-pyrolysis and co-combustion in TG [54–59].

Utilization of combustion characteristic factor S_N

Combustion characteristic factor S_N has been used to compare the combustion process for different fuel samples and under different oxygen concentrations.

Comparison of S_N for Baoji coal, sawdust and WCS is listed in Fig. 10, which shows that S_N of two biomass (sawdust and WCS) is much higher than that of Baoji coal, and the integral combustion characteristics of ignition and burnout for biomass is obviously better than that of coal, consistent with the results from Fig. 1. However, results of Fig. 10 also show that the S_N of sawdust is slightly higher than that of WCS, even Fig. 1 has demonstrated that the ignition of WCS is better. It is due to that S_N is an integral parameter considering both ignition and burnout, in Fig. 2 and Table 2 we have mentioned that the E and k_0 of sawdust is larger than that of WCS, which means the characteristics of reaction velocity and burnout is much faster than that of WCS. Consequently, the integral result of ignition and burnout is that the S_N is better for sawdust than WCS.

Effect of C_{O_2} on the S_N for WCS combustion is shown in Fig. 11. With the increase of C_{O_2}, it shows an exponential relationship ($S_N = 7.128 \times 10^{-9} \times \exp(C_{O_2}/0.368) - 6.126 \times 10^{-9}$) between S_N and C_{O_2}. As mentioned in

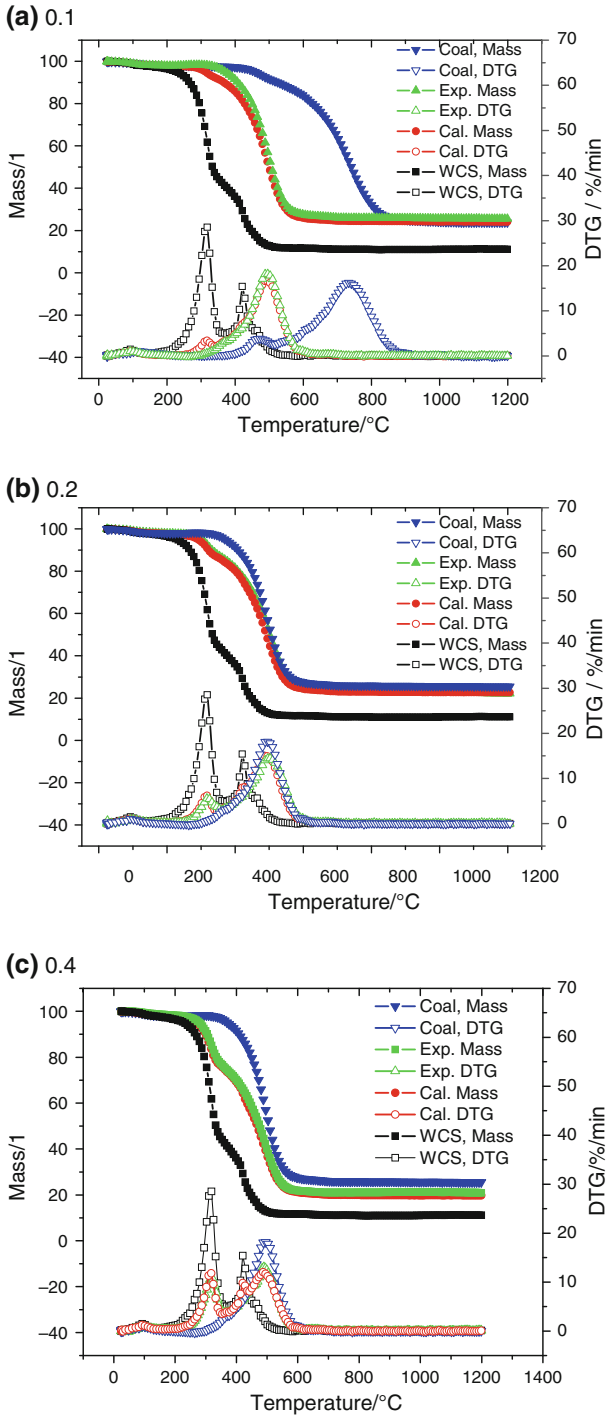

Fig. 9 Comparison of TG and DTG curves between experimental values and weighted average values for combustion of Baoji coal blended with WCS at different mixing ratios: 0, 0.1, 0.2, 0.4, 1 (β = 30 K min^{-1}; particle diameters = 198–450 μm; C_{O_2} = 0.2.)

Fig. 3 and Table 3 with C_{O_2} increasing, the peak value of DTG curve and reaction velocity increase but T_p decreases, leading to the exponential relationship finally.

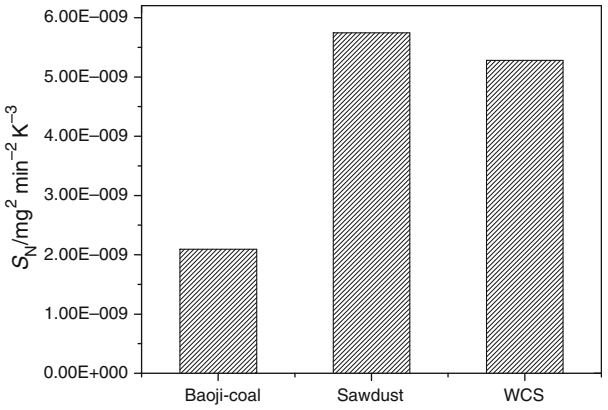

Fig. 10 Comparison of S_N for Baoji coal, sawdust and WCS (β = 30 K min^{-1}; particle diameters = 198–450 μm; C_{O_2} = 0.2.)

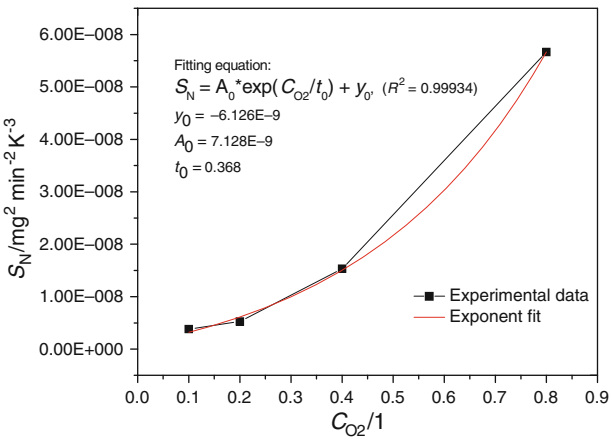

Fig. 11 Effect of C_{O_2} on S_N for WCS combustion

Conclusions

In this research, combustion kinetics of WCS is investigated using TG, compared with sawdust and Baoji coal; and the co-combustion of WCS with Baoji coal is also investigated. Coats-Redfern method is employed to determine the kinetics parameters, and combustion characteristic factor S_N is also applied to describe the process of WCS combustion. The conclusions are summarized as follows:

1. There are two peaks of mass loss (volatile combustion and char combustion) for combustion of WCS and only one peak for coal. The ignition characteristics of WCS is better than that of sawdust and coal, and the activation energy E of WCS-volatile combustion and WCS-char combustion are 78.55 and 44.59 kJ mol^{-1}, smaller than that of sawdust and coal combustion. However, the pre-exponential factor k_0 of WCS is much lower than that of sawdust, and then the burnout characteristic of WCS is worse than that of sawdust.

2. The heating rate and oxygen concentration C_{O_2} affect the combustion of WCS, but the effect of particle diameter is little. With the increasing in the heating rate, the ignition of WCS is delayed. The effect of oxygen concentration C_{O_2} is significant. With the increase of C_{O_2} from 0.1 to 0.8, the ignition of WCS is improved obviously, and the mass loss of first stage volatile combustion increases from 50 to 85%, when C_{O_2} reaches up to 0.8, the second DTG peak of char combustion would almost disappear. C_{O_2} affects the E and k_0 of volatile combustion largely, under the lean-oxygen condition there is no much change of E and k_0 for volatile combustion; however, when C_{O_2} continually increases from 0.2 to 0.4 and 0.8 under rich-oxygen condition, E has increased threefold and k_0 also intensively increases from 10^6 to 10^{13}–10^{22}. Oppositely, effect of C_{O_2} on the E and k_0 of heterogeneous char combustion is always little.
3. Application of combustion characteristic factor S_N illustrates that the integral combustion characteristics of ignition and burnout for biomass (sawdust and WCS) is obviously better than that of coal, and the S_N of WCS is a bit lower than that of sawdust. With the increase of C_{O_2}, there is an exponential relationship ($S_N = 7.128 \times 10^{-9} \times \exp(C_{O_2} /0.368) - 6.126 \times 10^{-9}$) between S_N and C_{O_2}.
4. All the DTG curves of co-combustion give two peaks, and the experimental and weighted-average curves coincide well under the thermogravimetric environment. With the increase of mixing ratio that WCS added, E and k_0 of volatile combustion increase, but correspondingly E and k_0 of char combustion decrease.

Acknowledgements The present work was supported by the Natural Science Funds of China (No. 50976086), ESPRC (EP/F061188/1), and China Scholarship Council.

References

1. Wang XB, et al. Nitrogen, sulfur, and chlorine transformations during the pyrolysis of straw. Energy Fuels. 2010;24:5215–21.
2. Dumanli AG, Tas S, Yurum Y. Co-firing of biomass with coals Part 1. Thermogravimetric kinetic analysis of combustion of fir (Abies bornmulleriana) wood. J Therm Anal Calorim. 2011; 103(3):925–33.
3. Wang X-B, Zhao Q-X, Tan H-Z. Kinetic analysis of nitric oxide reduction using biogas as reburning fuel. Afr J Biotechnol. 2009;8(10):2251–7.
4. Gonzalez-Diaz L, et al. Expert system for integrated plant protection in pepper (*Capsicum annuun* L.). Exp Syst Appl. 2009; 36:8975–9.
5. Kulkarni M, Phalke S. Evaluating variability of root size system and its constitutive traits in hot pepper (*Capsicum annum* L.) under water stress. Sci Hortic. 2009;120:159–66.
6. Yongxia H, Baoli Z, Xiaoling W. Allelopathy of decomposing pepper stalk on pepper growth. Chin J Appl Ecol. 2006;17(4): 699–702.
7. Wang X, et al. Experimental investigation on biomass co-firing in a 300 MW pulverized coal-fired utility furnace in China. Proc Combust Inst. 2011;33(2):2725–33.
8. Ulloa CA, Gordon AL, García XA. Thermogravimetric study of interactions in the pyrolysis of blends of coal with radiata pine sawdust. Fuel Process Technol. 2009;90:583–90.
9. Wei X, Lopez C, Puttkamer Tv. Assessment of chlorine-alkali-mineral interactions during co-combustion of coal and straw. Energy Fuels. 2002;16:1095–108.
10. Tan HZ, et al. Influence of metal elements on the evolution of CO and CH4 during the pyrolysis of sawdust. Afr J Biotechnol. 2010;9(3):331–9.
11. Morgana PA, Robertsona SD, Unswortha JF. Combustion studies by thermogravimetric analysis: 1. Coal Oxid Fuel. 1986;65(11): 1546–51.
12. Zhao Y, Hu H, Jin L. Pyrolysis behavior of weakly reductive coals from northwest China. Energy Fuels. 2009;23:870–5.
13. Ghetti P, Robertis UD, D'Antone S. Coal combustion: correlation between surface area and thermogravimetric analysis data. Fuel. 1985;64(7):950–5.
14. Suarez A, et al. Thermal analysis of the combustion of charcoals from *Eucalyptus dunnii* obtained at different pyrolysis temperatures. J Therm Anal Calorim. 2010;100(3):1051–4.
15. Niu SL, et al. Thermogravimetric analysis of combustion characteristics and kinetic parameters of pulverized coals in oxy-fuel atmosphere. J Therm Anal Calorim. 2009;98(1):267–74.
16. Ren Y, Freitag NP, Mahinpey N. A simple kinetic model for coke combustion during an in situ combustion (ISC) process. J Can Petrol Technol. 2007;46(4):47–53.
17. Ambalae A, Mahinpey N, Freitag N. Thermogravimetric studies on pyrolysis and combustion behavior of a heavy oil and its asphaltenes. Energy Fuels. 2006;20(2):560–5.
18. Zouaoui N, et al. Study of experimental and theoretical procedures when using thermogravimetric analysis to determine kinetic parameters of carbon black oxidation. J Therm Anal Calorim. 2010;102(3):837–49.
19. Kalogirou M, Samaras Z. Soot oxidation kinetics from TG experiments. J Therm Anal Calorim. 2010;99(3):1005–10.
20. Sancheza ME, et al. Thermogravimetric kinetic analysis of the combustion of biowastes. Renew Energy. 2009;34(6):1622–7.
21. Li X, Ma B, Xua L. Thermogravimetric analysis of the co-combustion of the blends with high ash coal and waste tyres. Thermochim Acta. 2006;441(4):79–83.
22. García AN, Font R, Esperanza MM. Thermogravimetric kinetic model of the combustion of a varnish waste based on polyurethane. Energy Fuels. 2001;15(4):848–55.
23. Zhaosheng Y, Xiaoqian M, Ao L. Thermogravimetric analysis of rice and wheat straw catalytic combustion in air- and oxygen-enriched atmospheres. Energy Convers Manag. 2009;50:561–6.
24. Zapata B, et al. Thermo-kinetics study of orange peel in air. J Therm Anal Calorim. 2009;98(1):309–15.
25. Yagmur S, Durusoy T. Kinetics of combustion of oil shale with polystyrene. J Therm Anal Calorim. 2009;96(1):189–94.
26. Ferdous D, Dalai AK, Bej SK. Pyrolysis of lignins: experimental and kinetics studies. Energy Fuels. 2002;16(6):1405–12.
27. Cloke M, Lester E, Leney M. Effect of volatile retention on products from low temperature pyrolysis in a fixed bed batch reactor. Fuel. 1999;78:1719–28.
28. Matham JG, Kandiyoti R. Coal pyrolysis yields from fast and slow heating in a wire-mesh apparatus with a gas sweep. Energy Fuels. 1988;2(4):505–11.
29. Buryan P, Staff M. Pyrolysis of the waste biomass. J Therm Anal Calorim. 2008;93:637–40.

30. Şahin Ö, Özdemir M, Aslanolu M. Calcination kinetics of ammonium pentaborate using the Coats-Redfern and genetic algorithm method by thermal analysis. Ind Eng Chem Res. 2001;40(6):1465–70.
31. Kok MV, Keskin C. Comparative combustion kinetics for in situ combustion process. Thermochim Acta. 2001;369(1):143–7.
32. Coats A, Redfern J. Kinetic parameters from thermogravimetric data. Nature. 1964;201:68–9.
33. Nie QH, Sun SZ, Li ZQ. Thermogravimetric analysis on the combustion characteristics of brown coal blends. J Combust Sci Technol. 2001;7(1):72–6.
34. Wang C, FengyinWang QirongYang. Thermogravimetric studies of the behavior of wheat straw with added coal during combustion. Biomass Bioenergy. 2009;33:50–6.
35. Tsamba AJ, Yang W, Blasiak W. Pyrolysis characteristics and global kinetics of coconut and cashew nut shells. Fuel. 2006; 86:523–30.
36. Liang XH, Kozinski JA. Numerical modeling of combustion and pyrolysis of cellulosic biomass in thermogravimetric systems. Fuel. 2000;79:1477–86.
37. Yu LJ, Wang S, Jiang XM. Thermal analysis studies on combustion characteristics of seaweed. J Therm Anal Calorim. 2008; 93(2):611–7.
38. Zhou L, Wang Y, Huang Q. Thermogravimetric characteristics and kinetic of plastic and biomass blends co-pyrolysis. Fuel Process Technol. 2006;87:963–9.
39. Sutcu H. Pyrolysis by thermogravimetric analysis of blends of peat with coals of different characteristics and biomass. J Chin Inst Chem Eng. 2007;38:245–9.
40. Orfao JJM, Antunes FJA, Figueiredo JL. Pyrolysis kinetics of lignocellulosic materials—three independent reactions model. Fuel. 1999;78:349–58.
41. Biagini E, Lippi F, Petarca L. Devolatilization rate of biomasses and coal-biomass blends: an experimental investigation. Fuel. 2002;81:1041–50.
42. Yang H, Yan R, Chen H. Characteristics of hemicellulose, cellulose and lignin pyrolysis. Fuel. 2007;86:1781–8.
43. McKendry P. Energy production from biomass (part 1): overview of biomass. Bioresour Technol. 2002;83:37–46.
44. Gani A, Naruse I. Effect of cellulose and lignin content on pyrolysis and combustion characteristics for several types of biomass. Renew Energy. 2007;32:649–61.
45. Janse AMC, de Jonge HG, Prins W. The combustion kinetics of char obtained by flash pyrolysis of pine wood. Ind Eng Chem Res. 1998;37:3909–18.
46. Varhegyi G, Meszaros E, Antal M. Combustion kinetics of corncob charcoal and partially demineralized corncob charcoal in the kinetic regime. Ind Eng Chem Res. 2006;45:4962–70.
47. Kashiwagi T, Nambu H. Global kinetic constants for thermal oxidative degradation of a cellulosic sample. Combust Flame. 1992;88:345–68.
48. Fang MX, Shen DK, Li YX. Kinetic study on pyrolysis and combustion of wood under different oxygen concentrations by using TG-FTIR analysis. J Anal Appl Pyrolysis. 2006;77:22–7.
49. Quan C, Li AM, Gao NB. Thermogravimetric analysis and kinetic study on large particles of printed circuit board wastes. Waste Manage. 2009;29(8):2353–60.
50. Chan WCR, Kelbon M, Krieger-Brockett B. Single-particle biomass pyrolysis: correlations of reaction products with process conditions. Ind Eng Chem Res. 1988;27(12):2261–75.
51. Encinar JM, et al. Pyrolysis of two agricultural residues: olive and grape bagasse. Influence of particle size and temperature. Biomass Bioenergy. 1996;11(5):397–409.
52. Zhang X, et al. Study on biomass pyrolysis kinetics. J Eng Gas Turbines Power. 2006;128(3):493–6.
53. Aboulkas A, et al. Pyrolysis kinetics of olive residue/plastic mixtures by non-isothermal thermogravimetry. Fuel Process Technol. 2009;90(5):722–8.
54. Vuthaluru HB. Investigations into the pyrolytic behaviour of coal/biomass blends using thermogravimetric analysis. Bioresour Technol. 2004;92(2):187–95.
55. Sonobe T, Worasuwannarak N, Pipatmanomai S. Synergies in co-pyrolysis of Thai lignite and corncob. Fuel Process Technol. 2008;89(12):1371–8.
56. Garc I, et al. Co-pyrolysis of sugarcane bagasse with petroleum residue. Part I: thermogravimetric analysis. Fuel. 2001;80(9): 1245–58.
57. Sharypov VI, et al. Co-pyrolysis of wood biomass and synthetic polymer mixtures. Part I: influence of experimental conditions on the evolution of solids, liquids and gases. J Anal Appl Pyrolysis. 2002;64(1):15–28.
58. Kastanaki E, Vamvuka D. A comparative reactivity and kinetic study on the combustion of coal-biomass char blends. Fuel. 2006;85(9):1186–93.
59. Haykiri-Acma H, Yaman S. Effect of biomass on burnouts of Turkish lignites during co-firing. Energy Convers Manag. 2009; 50(9):2422–7.